ELSEVIER

Bone 42 (2008) 332–340

BONE

www.elsevier.com/locate/bone

Autologous stem cell regeneration in craniosynostosis

Eduardo K. Moioli [a], Paul A. Clark [b], D. Rick Sumner [c], Jeremy J. Mao [a,*]

[a] *Columbia University, College of Dental Medicine, Tissue Engineering and Regenerative Medicine Laboratory, 630 W. 168 St. – PH7E CDM, New York, NY 10032, USA*

[b] *University of Wisconsin at Madison Hospital, Department of Neurological Surgery CSC K4/879, 600 Highland Ave., Madison, WI 53792, USA*

[c] *Rush University, Department of Anatomy and Cell Biology, 600 South Paulina, Suite 507, Chicago, IL 60612, USA*

Received 19 March 2007; revised 24 September 2007; accepted 1 October 2007
Available online 17 October 2007

Abstract

Craniosynostosis occurs in one of 2500 live human births and may manifest as craniofacial disfiguration, seizure, and blindness. Craniotomy is performed to reshape skull bones and resect synostosed cranial sutures. We demonstrate for the first time that autologous mesenchymal stem cells (MSCs) and controlled-released TGFβ3 reduced surgical trauma to localized osteotomy and minimized osteogenesis in a rat craniosynostosis model. Approximately 0.5mL tibial marrow content was aspirated to isolate mononucleated and adherent cells that were characterized as MSCs. Upon resecting the synostosed suture, autologous MSCs in collagen carriers with microencapsulated TGFβ3 (1ng/mL) generated cranial suture analogs characterized as bone–soft tissue–bone interface by quantitative histomorphometric and μCT analyses. Thus, surgical trauma in craniosynostosis can be minimized by a biologically viable implant. We speculate that proportionally larger amounts of human marrow aspirates participate in the healing of craniosynostosis defects in patients. The engineered soft tissue–bone interface may have implications in the repair of tendons, ligaments, periosteum and periodontal ligament.

Keywords: Tissue engineering; Tissue regeneration; Bone; Growth factor; TGFβ3

Introduction

Cell-based therapies have been considered as a key ingredient in the anticipated era of personalized medicine. In this context, diseased, ageing or traumatized tissues are to be replaced by the patient's own (autologous) cells, as opposed to analogous tissue grafts that require donor sites. Autologous tissue grafts, the current "gold standard", are harvested from patients for the reconstruction of defects resulting from trauma, chronic diseases, congenital anomalies, or tumor resection. Compared to autologous tissue grafts, a key advantage of cell-based therapies is to minimize donor site morbidity [1,2]. For example, a patient who has a bone graft harvested from the iliac crest for facial reconstruction experiences donor site morbidity of the iliac crest. Early attempts of therapeutic cell delivery adopted the concept that cells in diseased tissues were to be replaced by like cells that are healthy [1,2]. For example, degenerating arthritic cartilage was to be repaired by healthy chondrocytes. A number of drawbacks have become apparent in association with early attempts of autologous cell therapies. First, sufficient numbers of healthy donor cells are scarce, and cannot be obtained without large donor site trauma. A patient with cardiac infarct has few healthy cardiomyocytes to spare for the healing of the infarcted cardiac tissue. Second, delivered cells without carriers tend to migrate away from the intended location. For the regeneration of structural tissues such as bone or cartilage, cell delivery without carriers fails due to a lack of the needed structural support and mechanical strength. Third, the delivered lineage-specific cells, due to programmed cell death, necrosis, or loss of mitotic potential are often incapable of maintaining the long-term viability of the regenerating tissue.

Stem cells or progenitor cells may circumvent the current deficiencies of tissue regeneration by autologous tissue grafts or lineage-specific cells. For example, bone marrow content

* Corresponding author. Columbia University College of Dental Medicine, 630 W. 168 St. – PH7E CDM, New York, NY 10032, USA. Fax: +1 342 0199.
E-mail address: jmao@columbia.edu (J.J. Mao).

8756-3282/$ - see front matter © 2007 Elsevier Inc. All rights reserved.
doi:10.1016/j.bone.2007.10.004

can be aspirated to isolate mesenchymal stem cells (MSCs) that retain multipotency following a number of population doublings [1,2]. MSCs can differentiate into multiple cell lineages such as osteoblasts, adipocytes, chondrocytes, cardiomyocytes and myoblasts [3–5], thus providing the possibility that a common cell source can heal a number of tissues, as opposed to harvesting a healthy tissue to heal like tissue with autologous grafting. MSCs or MSC-derived cells have been seeded in biocompatible scaffolds, and shaped into target anatomical structures [6–9]. An important clue from these studies is the importance of the manipulation of cell fate in scaffold carriers.

Craniosynostosis occurs in one of 2500 live human births and represents the premature ossification of one or more cranial vault sutures [10–12]. In the first few postnatal years, rapid brain growth under the abnormally high intracranial pressure in the craniosynostosis patient results in disfigured cranial and facial bones, in addition to a variety of neurological disorders such as blindness, deafness and seizure. The microscopic characteristics of craniosynostosis include the premature ossification of the involved cranial sutures, which, under normal conditions, remain patent and permit expansive growth of calvarial bones along with the enlargement of the brain [10,13]. Craniotomy is the only treatment choice for craniosynostosis [14]. In a traumatic and complex surgery, calvarial bones are surgically removed, reshaped and re-attached after the resection of the synostosed cranial sutures [15]. Post-surgical, secondary synostosis may occur partially due to the abnormally high osteogenic potential of the synostosed cranial suture [16]. Synostosed human cranial sutures have significantly higher osteogenic potential than non-synostosed cranial sutures: approximately 50% higher bone formation rate and up to 75% higher osteogenic differentiation rate [16], thus necessitate controlled osteogenesis post-intervention.

Transforming growth factor β3 (TGFβ3) has been found to inhibit the ossification of synostosing cranial sutures [10,17–19]. Syndromic craniosynostosis such as Crouzon syndrome is associated with substantial decrease in TGFβ3 activity in sutural fibroblasts [10,20]. The decrease in TGFβ3 activity corresponds to increased bone formation rate, suggesting that TGFβ3 function, if restored, may counteract sutural synostosis. TGFβ3 soaked in collagen gel delays the synostosis process in the synostosing rat suture or an induced rabbit synostosis model [17,18]. However, previous work has not been designed to explore whether the level of surgical trauma of craniosynostosis can be reduced by a biologically derived cranial suture replacement and is not applicable to post-symptomatic cases since these approaches target the fusing suture before synostosis occurs. Currently, upon the resection of the synostosed cranial suture, a bony defect is created without a biologically derived or synthetic implant, leading to clinically observed secondary synostosis. Furthermore, growth factor delivery without controlled release results in relatively rapid denature and diffusion [21]. Recently, we developed a strategy of controlled release of microencapsulated TGFβ3 from biocompatible microspheres, and further tested effective sterilization modalities for microspheres without substantial effects on the encapsulated growth factor [22]. In the present study, we first isolated autologous MSCs from approximately 0.5mL bone marrow aspirates in the rats whose posterior interfrontal sutures (PIF) are synostosed during postnatal 10 to 21 days [10,23]. Autologous MSCs co-seeded with microencapsulated TGFβ3 in collagen carrier generated a cranial suture analog (maintenance of fibrous tissue versus bone) after localized osteotomy of the synostosed PIF suture in the same rat that had earlier donated the bone marrow sample. Image-based, histological and immunohistological assessments of the engineered cranial sutures demonstrated a biologically derived bone–soft tissue–bone interface. Without autologous MSCs and control-released TGFβ3, secondary synostosis readily occurred in the resected PIF osteotomy site. This study represents a rare demonstration of biological replacement of a complex anatomic structure in an *in vivo* model using autologous stem cell and drug delivery approaches.

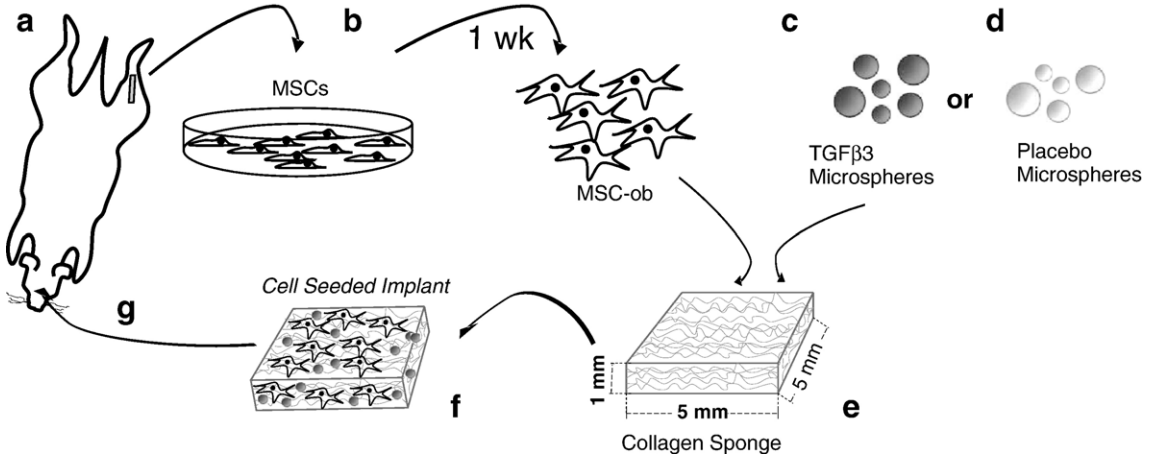

Fig. 1. Fabrication of autologous stem cell-based implants with controlled delivery of TGFβ3. Aspiration of autologous bone marrow (a) and isolation of mononucleated and adherent cells that will populate the engineered cranial suture (b). (c) Differentiation of MSCs into cells of several tissue-specific lineages including osteoblasts. (d) Encapsulation of TGFβ3 in poly(DL-lactic-co-glycolic acid) (PLGA) microspheres that are biocompatible and biodegradable for controlled release. (e) and (f) Loading of microencapsulated TGFβ3 (e) and autologous cells (f) in a biocompatible collagen sponge carrier. (g) Implantation of engineered construct into the osteotomy site of synostosed cranial suture in the same corresponding rat that earlier donated bone marrow sample.

Materials and methods

Bone marrow aspiration and culture

Implant fabrication, from bone marrow aspiration to implantation, is outlined in Fig. 1. Six-week-old, male Sprague–Dawley rats were weighed and anesthetized with inhalant isofluorane. The skin in the anterior proximal tibia region was clipped of hair, and disinfected with Povidone Iodine and 70% alcohol. A spinal needle was inserted into the tibial marrow cavity to aspirate up to 0.5mL marrow content with or without a small skin incision (Fig. 2a). The aspirated bone marrow was mechanically disrupted by successive passages through, 18-, 20- and 25-gauge needles, re-suspended in DMEM/FBS/antibiotics, and plated for 1week to isolate mononucleated, adherent cells (Figs. 1c and 2b). The mononucleated and adherent cells underwent rapid proliferation (Figs. 1c and 2c), and when reaching 80–90% confluence, were trypsinized, counted, and seeded at approximately 5×10^4 cells/dish for further expansion. All bone marrow cell cultures were incubated in 95% humidity/5% CO_2 at 37 °C in Dulbecco's Modified Eagle's Medium (DMEM) with 10% FBS (Biocell, Rancho Dominguez, CA) and 1% antibiotics (1X Antibiotic–Antimycotic, including 100 units/mL Penicillin G sodium, 100 μg/mL Streptomycin sulfate and 0.25 μg/mL amphotericine B (Gibco, Invitrogen, Carlsbad, CA). In all rats, bone marrow aspiration was well tolerated without any complications such as infections or weight loss. All experimental procedures were approved by the institutional IACUC.

Multi-lineage differentiation

Following the observation of the growth capacity of the isolated mononucleated adherent cells, we examined their multi-potentiality. Culture-expanded adherent and mononucleated cells were differentiated into osteogenic, chondrogenic and adipogenic cells per our prior methods [6,24]. Osteogenic differentiation was induced by medium supplements of 100 nM dexamethasone, 0.05 mM ascorbic acid and 100 mM β-glycerophosphate [22,24,25]. All differentiation media were changed every 3–4 days. Von Kossa mineral staining was used to visualize mineral matrix deposition, whereas calcium levels were determined in lysed samples using calcium reagent (RaiChem, San Diego, CA). Chondrogenic differentiation was induced by supplements of 1% 1X ITS+ (insulin–transferring–sodium selenite), 100 μg/mL sodium pyruvate, 50 μg/mL ascorbate, 40 μg/mL L-proline, 0.1 μM dexamethasone, and 10 ng/mL TGFβ3 [24,25]. Alcian blue was used to label glycosaminoglycans in chondrogenic culture. Glycosaminoglycan (GAG) content was determined biochemically from lysed chondrogenic cultures using GAG detection kit (Glyscan, Westbury, NY). Adipogenic differentiation was induced by 1 μM dexamethasone, 60 μM indomethacin, 500 μM IBMX (3-Isobutyl-1-methylxanthine), and 10 μg/mL insulin [26]. Lipid formation was determined by Oil-red O staining [26].

Controlled release of microencapsulated TGFβ3

Microspheres of 50:50 copolymer ratio of poly(DL-lactic-co-glycolic acid) (PLGA; Sigma, St. Louis, MO) encapsulating recombinant human TGFβ3 (R&D Systems, Minneapolis, MN) were fabricated using the double-emulsion technique ((water-in-oil)-in-water) per our prior work [22]. Briefly, PLGA (250 mg) was dissolved into 1mL dichloromethane. A total of 2.5 μg TGFβ3 was diluted in 50 μL of 4mM HCl–0.1% bovine serum albumin (BSA) solution and added to the PLGA solution, forming a mixture (primary emulsion) that was emulsified for 1 min (water-in-oil). A secondary emulsion was obtained by adding 2 mL of 1% polyvinyl alcohol (w/v) (PVA, MW 30,000–70,000) and mixed for 1 min ((water-in-oil)-in-water). Finally, 100 mL of 0.1% PVA solution (w/v) was added to the mixture and stirred for 1 min using an electric stirrer at 450 rpm followed by the addition of 100 mL of 2% isopropanol (v/v). Placebo PLGA microspheres were fabricated in the same fashion but encapsulated distilled water. Lyophilized microspheres were sterilized with ethylene oxide gas for 24 h, which we earlier found to effectively sterilize PLGA microspheres encapsulating growth factors without substantial effects on either release profile or bioactivity [22]. PLGA microspheres encapsulating distilled water or TGFβ3 were infused in collagen carriers and incubated in 1% BSA up to 4 weeks at 37 °C in water bath in order to determine the release profile of TGFB3 from the fabricated implants. TGFβ3 was detected in supernatant by a TGFβ3 ELISA detection kit per manufacturer protocol (R&D Systems, Minneapolis, MN).

Effects of control-released TGFβ3 on osteogenic differentiation of MSCs

Human mesenchymal stem cells isolated from bone marrow (AllCells, Berkeley, CA) were cultured in 6-well plates (3×10^4 cells/well) with osteogenic supplements as described above and incubated with TGFβ3-encapsulated

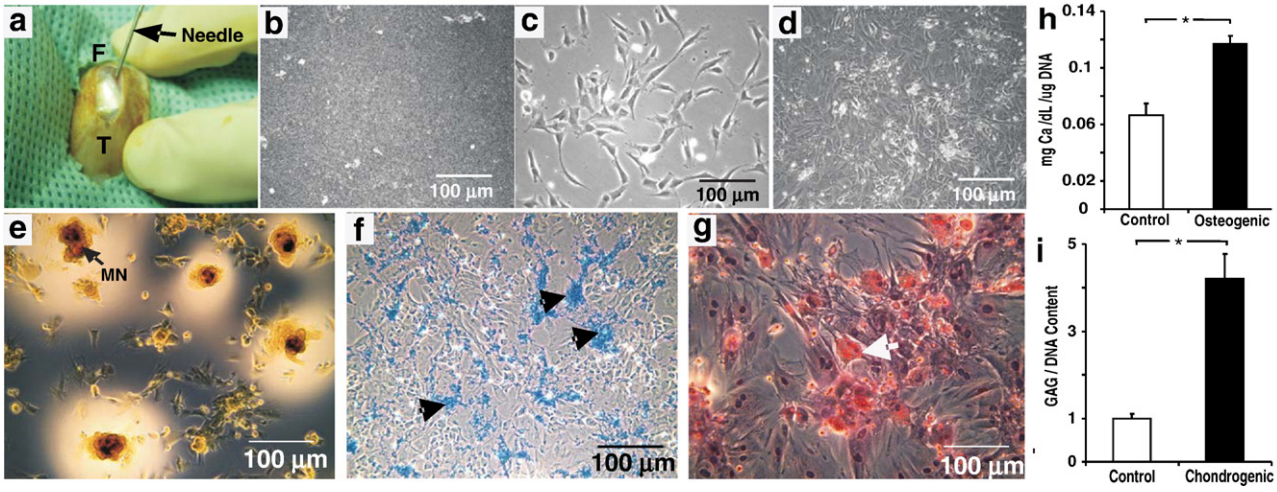

Fig. 2. Bone marrow aspiration and isolation of mononucleated adherent cells. (a) Marrow aspiration from rat tibia (T) with a spinal needle. F: femur. (b) Marrow content plated after mechanical disruption. (c) Mononucleated adherent cells after 7-day culture showing spindle shape, typical of mesenchymal stem cells (MSCs). (d) Mononucleated and adherent cells undergo rapid growth and become confluent. Differentiation of mononucleated and adherent cells into multiple lineages including osteoblast-like (e), chondrocyte-like (f), and adipocyte-like (g) cells. e. Von Kossa stain of mineral nodule (MN) formation after 4 week exposure to osteogenic supplements (details in text). (f) Alcian blue staining of a proteoglycan rich matrix (black arrowheads) after 4 week exposure to chondrogenic supplements (details in text). (g) Oil-red O staining of intracellular lipid vacuoles (white arrowhead) after 4 week exposure to adipogenic supplements (details in text). (h) Calcium content of osteogenic culture of rat bone marrow-derived MSCs versus control (no osteogenic supplements) culture. (i) Glycosaminoglycan (GAG) content of chondrogenic culture of rat bone marrow-derived MSCs versus control (no chondrogenic supplements) culture.

PLGA microspheres in transwell inserts at concentrations of 0, 0.035, 0.135, and 1.35 ng/mL of release in the first week. Cultures were fixed with 10% formalin and visualized with alkaline phosphatase and von Kossa stains to determine the level of osteogenic differentiation [22].

Preparation of in vivo implants

Four to six weeks were required for the subculture and expansion of the harvested MSCs [6, 22]. Pre-sized, and pre-wetted collagen sponge carriers ($5\times5\times1$ mm^3) (Helistat, Plainsboro, NJ) were seeded with cells at 5×10^6 cells/mL under light vacuum [12]. (Fig. 1e, f). TGFβ3 encapsulated or placebo PLGA microspheres (3mg) were loaded into MSC seeded collagen sponges to complete construct fabrication (Fig. 1f).

Rat craniosynostosis model and surgical procedures

The posterior interfrontal (PIF) suture is synostosed between postnatal 10 to 21 days in Sprague–Dawley rats, whereas all other cranial sutures are patent for life [10,18,23,27]. This is the closest anatomical model to human craniosynostosis at a scale that cranial surgery as in the present study can be performed. A small number of mouse genetic models of craniosynostosis have been recently reported [11,28,29], but the small size of mice prevents the present surgical manipulations. We performed osteotomy of the synostosed PIF suture to simulate the resection of synostosed sagittal suture (Fig. 1f), but avoided the removal and reshaping of other calvarial bones as in craniosynostosis patients, thus creating a model to minimize craniosynostosis surgery. Following disinfection, a midline incision was made along the mid-sagittal line of the skull, followed by deflection of the skin and subcutaneous tissue. The periosteum was deflected using a periosteal elevator, exposing the interfrontal, sagittal and coronal sutures. A full thickness osteotomy site (5×5 mm^2) was created with a dental burr under constant saline irrigation (Figs. 1g and 4a). The dura mater was kept intact, as in craniosynostosis surgeries.

Biological replacement of synostosed cranial suture

Autologous MSC and TGFβ3-loaded or placebo microsphere-loaded collagen carriers were implanted into the osteotomy site in each of corresponding rats that had earlier donated bone marrow samples (Figs. 1g and 4b). Four weeks after implantation, all rats were euthanized with CO_2, followed by *en bloc* harvest of calvarial bones including the osteotomy site.

Histology, immunohistochemistry, histomorphometry, and μCT

The retrieved calvarial samples were immediately fixed in 10% paraformaldehyde and imaged by μCT (ViVa CT 40, Scanco, Switzerland) with multiple slices at 21 μm resolution. Threshold values were determined from histograms of reconstructed images based on the valley between the bone voxel and soft tissue voxel peaks. Specimens were demineralized in equal volumes of 20% sodium citrate and 50% formic acid, subsequently embedded in paraffin, sectioned in the transverse plane at 5 μm thickness and stained with hematoxylin and eosin [23]. Sequential sections were immunoblotted for bone sialoprotein (BSP II) and osteopontin (OPN) for visualizing the extent of osteogenesis in the engineered cranial suture post-implantation [6]. Computerized histomorphometric analysis was performed to quantify bone volume and total tissue volume using our previously developed method of grid analysis by laying grids over microscopic specimens in 1175×880 μm^2 fields [30].

Statistical analysis

Numerical data for bone volume per total tissue volume (BV/TV), calcium content, and glycosaminoglycan (GAG) content were subjected to non-parametric Kruskal–Wallis tests with α level at 0.05.

Results

Up to 0.5 mL of bone marrow was aspirated from the rat tibial medullary cavity with a small incision in the anterior tibial region under sterile conditions (Fig. 2a). We subsequently simplified the bone marrow aspiration procedure by inserting the syringe needle directly into the marrow cavity without skin incision, and obtained comparable cell yield. The isolated bone marrow samples were tagged according to their corresponding donor rats for later autologous implantation, and were immediately plated as shown in Fig. 2b. Mononucleated and adherent cells were isolated within 1week and showed typical spindle-like morphology similar to that of mesenchymal stem cells (Fig. 2c) [6,24]. The mononucleated and adherent cells underwent rapid proliferation within 2–4 weeks of culture expansion (Fig. 2d). To demonstrate their multi-potentiality, mononucleated and adherent cells were treated with osteogenic, chondrogenic or adipogenic supplements, as described in detail above, and began to show lineage-specific differentiation within 4 weeks by von Kossa (in osteogenic culture) (Fig. 2e), Alcian blue (in chondrogenic culture) (Fig. 2f), and Oil-red O (in adipogenic culture) (Fig. 2g) stains. Quantitative analyses confirmed the significantly higher calcium content in the derived osteoblasts (Fig. 2h), and significantly higher glycosaminoglycan content in the derived chondrocytes (Fig. 2i). Thus, bone marrow aspirated, mononucleated and adherent cells, now deemed to contain MSCs [6,24], are capable of differentiating into multiple cell lineages, even from 0.5 mL of marrow content.

Microspheres fabricated by the double-emulsion approach from poly(DL-lactic-co-glycolic acid) (PLGA), a biocompatible material that undergoes hydrolysis *in vivo*, are shown in Fig. 3a. Per our prior methods [22], we encapsulated recombinant human TGFβ3 in PLGA microspheres (arrows in Fig. 3b) and infused TGFβ3-encapsulated microspheres or placebo microspheres in a collagen carrier (Fig. 3b). The *in vitro* release profile of TGFβ3 is shown in Fig. 3c, suggesting that microencapsulated TGFβ3 is continuously released up to the tested 28 days. Non-cumulative release of TGFβ3 is expressed as the released concentration per volume of implant (25 mm^3) in Fig. 3c. After the first week burst release in collagen carrier, approximately 1 ng/mL of TGFβ3 was released from PLGA microspheres at each observed time point up to the tested 28 days. The remaining encapsulated TGFβ3 is anticipated to be further released from the total encapsulation amount per our previous work [22].

We further tested whether control-released TGFβ3 was capable of attenuating the osteogenic differentiation of MSCs *in vitro*. MSCs isolated from commercially purchased human bone marrow samples were differentiated into osteogenic cells per detailed methods described below and in our previous work [6,24,25]. Upon incubation with placebo PLGA microspheres without TGFβ3, MSCs readily underwent osteogenic differentiation in the observed 14, 21 and 28 days, shown as progressively intense alkaline phosphatase and von Kossa staining (Fig. 3d, h, l). In contrast, MSCs incubated with TGFβ3 encapsulated in PLGA microspheres showed remarkable attenuation of osteogenic differentiation in a dose response

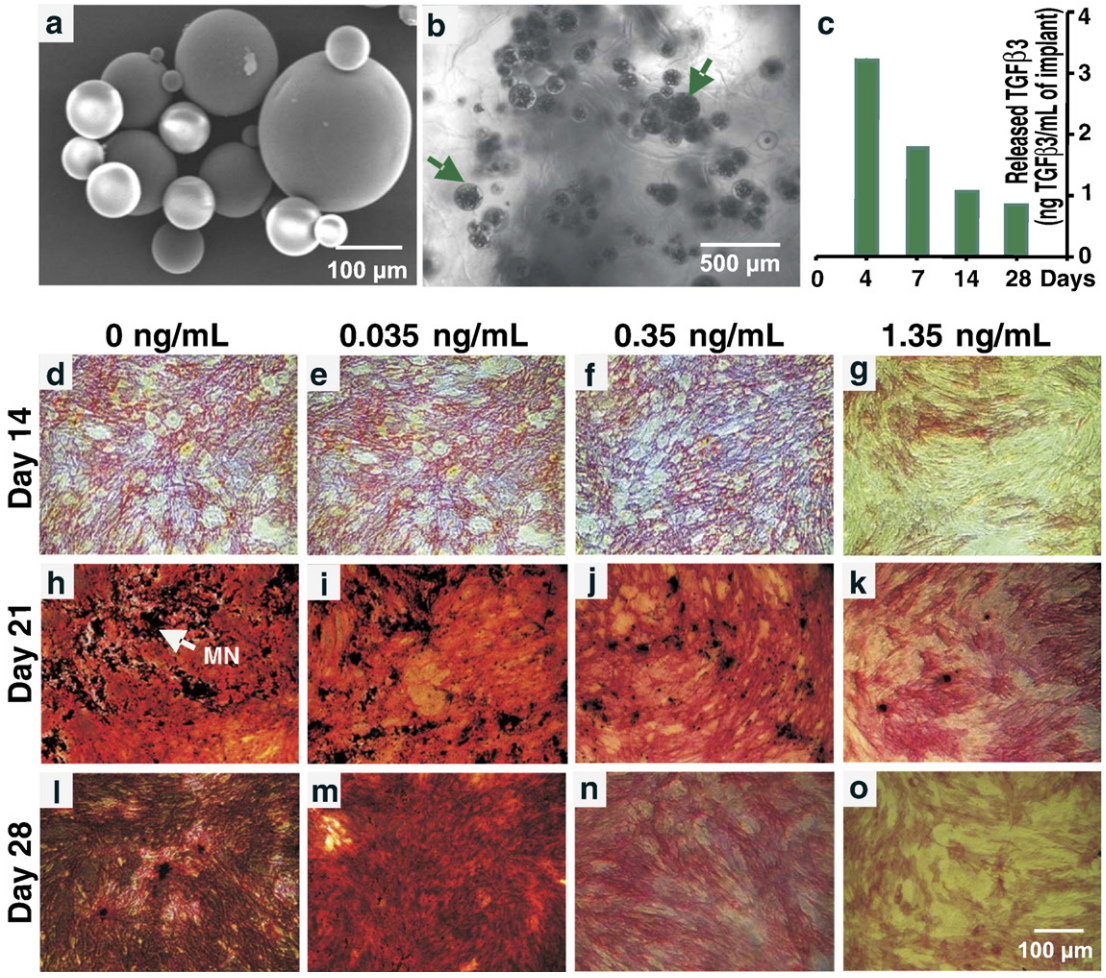

Fig. 3. TGFβ3 control-released from microencapsulation regulates mesenchymal stem cells (MSCs) *in vitro*. (a) Scanning electron micrograph (SEM) of fabricated poly (DL-lactic-co-glycolic acid) (PLGA) microspheres encapsulating TGFβ3 showing intact spherical surface morphology. (b) PLGA microspheres (green arrows) incorporated in collagen carrier. (c) *In vitro* release profile of TGFβ3 from PLGA microspheres in collagen carrier expressed as released TGFβ3 per unit implant volume (ng/mL) per week up to the tested 28 days. Osteogenic differentiation of MSCs progressed as increased alkaline phosphatase (red) and von Kossa (black) stainings (MN = mineral nodule) (d, h and i). Controlled release of TGFβ3 at multiple doses attenuated the osteogenic differentiation of MSCs with increasingly pronounced effects at the dose of 1.35 ng/mL for the tested 28 days (e–f, i–k, and m–o). Alkaline phosphatase and von Kossa staining (d through o).

manner among the tested 0.035 ng/mL (Fig. 3e, i, m), 0.35 ng/mL (Fig. 3f, j, n) and 1.35 ng/mL TGFβ3 (Fig. 3g, k, o) at the tested 14, 21, and 28 days *in vitro*. Accordingly, 1.35 ng/mL was selected for *in vivo* TGFβ3 delivery dose, given its most robust attenuation of osteogenic differentiation of MSCs (Fig. 3g, k, o).

The rat posterior interfrontal suture (PIF) undergoes synostosis between postnatal days 10 and 21, whereas all other rat cranial sutures remain patent for prolonged time [27]. This *in vivo* model has been adopted frequently in studies of craniosynostosis [10,18,23,31]. Localized osteotomy of the synostosed rat posterior interfrontal suture (PIF) was performed with details described above (Fig. 4a). Note that the anterior interfrontal suture (white arrow in Fig. 4a) and coronal suture (yellow arrow in Fig. 4a) remained intact. The dura mater was kept intact, thus eliminating the dura as a variable for both control and experimental groups. Although the dura mater has strong influence on the patency of cranial sutures [1,2,4,24,32], the present study was not designed to address the intricacies of dura mater biology. In craniosynostosis surgery, the dura mater is also kept intact [1,2,4,24,32]. Autologous MSCs co-seeded with microencapsulated TGFβ3 or placebo microspheres in collagen carriers (black arrow in Fig. 4b) were implanted in the suturectomy sites of corresponding rats that had earlier donated bone marrow samples ($N=4$). Four weeks following *in vivo* implantation, microscopic sections of the harvested calvarial samples showed increased re-synostosis in groups implanted with placebo PLGA microspheres ($N=4$) (Fig. 4c), demonstrating the remarkably strong osteogenic environment in the synostosed rat PIF suture even after sutural resection. In contrast, autologous MSCs with control-released TGFβ3 generate a bone–soft tissue–bone interface in the localized osteotomy site of the synostosed PIF suture in the same rats that earlier donated bone marrow samples ($N=4$) (Fig. 4d). Immunohistochemical analysis revealed marked and continuous expression of both bone sialoprotein (BSP II) and osteopontin (OPN) in the re-synostosed PIF osteomy site treated with placebo microspheres (Fig. 4e, g). In

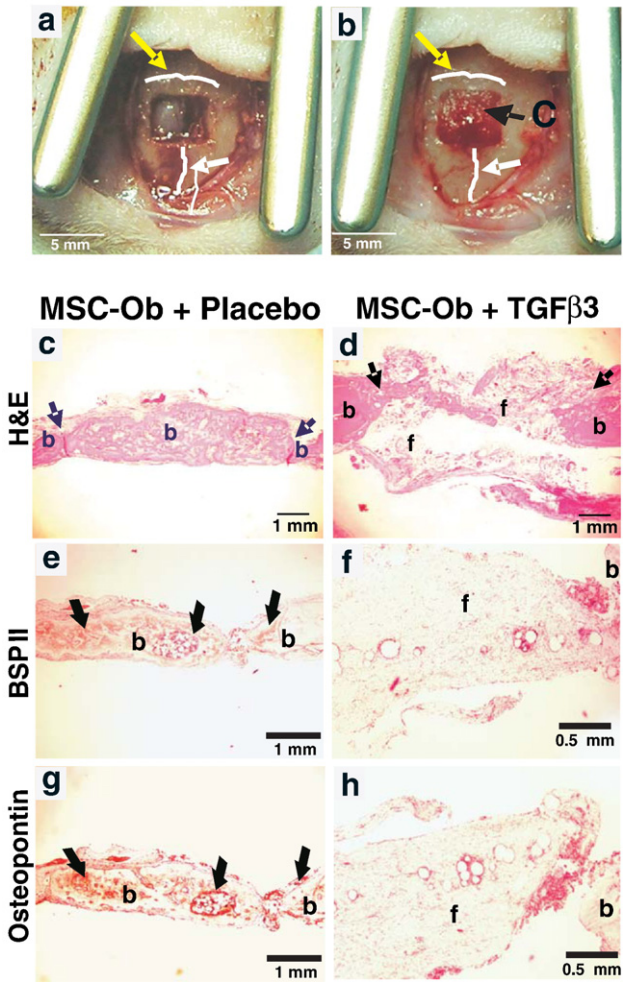

Fig. 4. Localized osteotomy of synostosed cranial suture and replacement with engineered construct. (a) Osteotomy of the synostosed rat posterior interfrontal (PIF) suture. The coronal suture (yellow arrow), and the anterior interfrontal suture (white arrow) are not ossified, per our previous work (23) and were kept intact during surgery. Dura mater was kept intact as in craniosynostosis surgery, thus eliminating the dura as a variable for both control and experimental groups. (b) Implantation of autologous MSCs and microencapsulated TGFβ3 in a collagen carrier in the resected PIF suture. (c) H&E staining showing secondary synostosis 4 weeks after the implantation of a control collagen carrier consisting of autologous MSCs and placebo PLGA microspheres, simulating post-surgical re-synostosis following craniosynostosis surgery. (d) H&E staining showing the formation of a cranial suture analog from autologous MSCs and TGFβ3 delivery, as characterized by a soft tissue interface (STI) between mineralized bone (b) (arrows pointing to the border of new bone formation fronts). Marked expression (dark brown stain) of bone sialoprotein II (BSP II) and osteopontin (OPN) in re-synostosed cranial suture implanted with a placebo treated implant (e and g). In contrast, BSP II and OPN, two late osteogenesis markers, were not immunolocalized to the engineered soft tissue interface (STI), but showed expression in the newly formed bone (b) in the osteotomized PIF suture treated with autologous MSCs and control-released TGFβ3 (f and h).

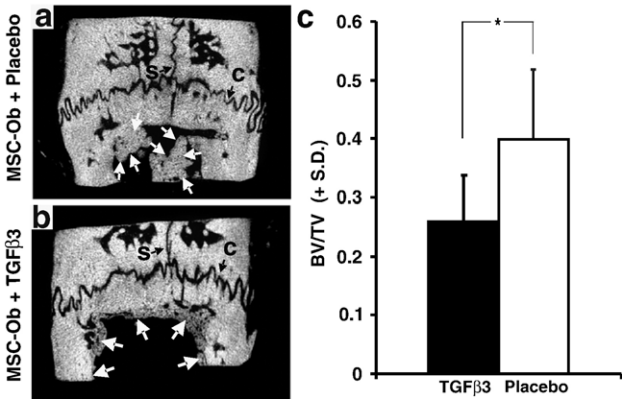

Fig. 5. Regulation of post-surgical synostosis in the engineered cranial suture. a. Microcomputed tomography (μCT) showing substantial progression of re-synostosis characterized as newly formed bone and mineralization (white arrows) in the resected cranial suture osteotomy site implanted with a placebo PLGA carrier after 4 weeks (c: coronal suture; s: sagittal suture). b. Secondary synostosis was substantially curbed upon the implantation of autologous MSCs and control-released TGFβ3 in a collagen carrier after 4 weeks. c. Quantification of new bone volume over total tissue volume (BV/TV) by computerized histomorphometric analysis showing significantly more mineralization in osteotomized synostosis suture healed with autologous MSCs and placebo collagen carriers than autologous MSCs and control-released TGFβ3 collagen carriers ($P<0.05$).

contrast, there was little BSP and OPN expression in the engineered soft tissue interface by autologous MSCs loaded with control-released TGFβ3, with the exception of marked BSP and OPN expression in surrounding bone (Fig. 4f, h).

Microcomputed tomography revealed the progression of remarkable mineralization in the resected PIF osteotomy site implanted with placebo PLGA microspheres (Fig. 5a). Alternately, implants of autologous MSCs and control-released TGFβ3 in collagen carriers substantially attenuated osteogenesis in the osteotomy site of synostosis, and generated an area of radiolucency that corresponds to the soft tissue interface in Fig. 4d, f and h, indicating that secondary synostosis has been substantially curbed (Fig. 5b). Quantitative analysis of the amount of mineralized tissue formation in the osteotomized synostosis sites by computerized histomorphometry revealed that autologous MSCs loaded with control-released TGFβ3 significantly reduced the amount of new bone volume over total tissue volume (BV/TV) (Fig. 5c), suggesting that autologous MSCs loaded with control-released TGFβ3 substantially attenuates an otherwise strong synostosis process.

Discussion

The present findings represent the first demonstration of a regenerated cranial suture from autologous stem cells, and the replacement of a synostosed cranial suture in an *in vivo* model. A biologically viable cranial suture may reduce surgical trauma from craniotomy of multiple calvarial bones in craniosynostosis patients, to localized osteotomy. Another potential advantage is that a biologically viable cranial suture may accommodate subsequent craniofacial growth by inhibiting the clinically observed adverse secondary synostosis after the resection of the synostosed cranial suture.

The present system is potentially applicable to the regeneration of other interface structures such as ligament–bone interface, tendon–bone interface, dentin–pulp interface, periodontal ligament–bone interface and periosteum–bone

interface, all with the common characteristics of bone–soft tissue interface. For example, the present TGFβ3 delivery and controlled release may be useful in ligament regeneration in which ectopic bone formation has been found in the intended ligament portion [33]. The field of tissue engineering to date has focused primarily on single tissues such as skin, bone, muscle or cartilage. In reality, the regeneration or *de novo* formation of diseased or traumatized tissues requires the constitution of multiple cell lineages. Once two or more cell types are manipulated in a tissue regeneration process, an interface is created such as the osteochondral interface [6,25,34,35] or the present fibro–osseous interface [36,37]. In these increasingly complex systems, autologous stem cell delivery and/or controlled release of signaling cues may be necessary for engineering the needed interface that segregates two or more different tissue phenotypes [38].

One of the primary concerns of autologous stem cell therapies is the lengthy time from cell harvest to the availability of a cell-based implant. In this study, a total of 4 to 6 weeks was needed to expand autologous MSCs from 0.5 mL bone marrow aspirates. Bone marrow contains highly heterogeneous cell populations [1,2,4,24,32], and only a fraction of the cells in the 0.5 mL bone marrow aspirate are MSCs. It is therefore remarkable that autologous MSCs can be expanded to a pre-defined cell density of 5×10^6 cells/mL, which we previously found to be sufficient for generating relatively large engineered structures [4,6,25]. The young rat age (6 weeks old) may be responsible for the relative high yield of MSCs in this study, and may be instructional towards the isolation of MSCs from young children who suffer from craniosynostosis. The rationale for TGFβ3 delivery is to counteract the abnormally high osteogenic potential in the synostosed cranial sutures such as in craniosynostosis patients [16]. Second, fabrication of PLGA microspheres and subsequent TGFβ3 encapsulation can be accomplished in several hours. Our previous work on the release profile of TGFβ3 and optimal sterilization technique for encapsulated growth factors indicates that the encapsulation of bioactive factors using biocompatible microspheres are ready for *in vivo* applications [22]. Although the human synostosis defects are much larger, more bone marrow contents can be obtained from the patient (up to 100 mL or so). Cell seeding in collagen carriers and the loading of TGFβ3 microspheres were also performed within hours. Given that craniosynostosis is an elective surgery, it appears that all presently performed procedures can be staged within a few weeks following the harvest of bone marrow sample, and completed within a reasonable time frame for clinical applications.

Certain craniosynostosis cases are linked to genetic mutations of FGFRs, MSX2, and TWIST [39]. We took into consideration of a rarely addressed question that host cells isolated for autologous cell therapies may carry the same genetic defects which have led to the anomalies in the first place. When autologous cells are applied to regenerate cranial sutures in craniosynostosis patients, a valid concern is that the isolated host cells may carry the same genetic defects and lead to post-surgical, secondary synostosis. In our previous work we observed progressive re-synostosis of a surgically created fibrous tissue interface in an ectopic rabbit calvarial model [12]. The presently demonstrated *in vivo* attenuation of an otherwise post-surgical re-synostosis by TGFβ3 suggests that growth factor delivery may serve as an effective approach to mediate strong synostosis potential of autologous cells in craniosynostosis. Following the delivery of microspheres in the *in vivo* model, the encapsulated TGFβ3 is likely released as PLGA microsphere shells undergo degradation. Controlled release is an advantageous approach for drug delivery because it circumvents shortcomings of bioactive factors delivered as free molecules, such as rapid denaturing and diffusion [4,24,30,40]. Although the *in vivo* release profile of a growth factor is difficult to measure, the presently observed attenuation of post-surgical mineralization in the resected synostosis model suggests that control-released TGFβ3 has been effective *in vivo*. We plan to track the released TGFβ3 by peptide labeling with radio label [4,24,40] or quantum dots [4,24,40] in follow-up experiments, and co-localize TGFβ3 and effector cells in the engineered cranial suture. Another important rationale for controlled release of TGFβ3 is to induce potential homing of cells that elaborate extracellular matrix molecules without a strong mineralization potential [4,24,40]. The cranial suture and the underlying dura mater consist of highly heterogeneous cell populations, with osteoblasts lining the bone formation fronts, fibroblastic or mesenchymal cells within the suture, etc. [13,41–44]. Sutural and dura mater cells have the potential to differentiate into osteoblasts [4,24,40,43] which is not favorable for the regeneration of a cranial suture in the treatment of craniosynostosis. Additional studies will address if control-released TGFβ3 induces the homing of fibroblastic and/or mesenchymal cells. Besides TGFβ3, other osteogenesis inhibiting molecules and signaling cues such as noggin and FGF-2 should also be explored with regard to their applications in counteracting craniosynostosis [45–48].

This study utilizes a multitude of technical approaches not only in the evaluation of the outcome of the regeneration of a complex anatomic structure by autologous bone marrow stem cells, but also biological and engineering approaches as therapeutic tools in a craniosynostosis model. A number of critical questions arise from the present findings and warrant additional studies. Cell labeling is necessary for delineating the relative contribution of delivered and locally resident cells to the regeneration of cranial sutures. We have begun to explore cell labeling with fluorescent proteins and/or quantum dots [4,24,40]. Several isolated genetic mouse models of craniosynostosis have been recently introduced [19,28,49,50]. Improved characterization, yield and survival are necessary prior to cell-based replacement of synostosed cranial sutures in genetic mouse models. A number of pending issues can be further addressed, such as whether the same genetic defects are present in autologous stem cells, or whether controlled release of TGFβ3 is critical to the regeneration of an engineered cranial suture analog [51,52]. In summary, our current findings represent a rare demonstration of the regeneration of a complex tissue in an *in vivo* animal model from autologous stem cells via the aspiration of 0.5 mL of bone marrow content. It appears that proportionally larger amounts of human bone marrow aspirates (up to 100 mL) may be sufficient for the regeneration of proportionally larger craniosynostosis defects in patients.

Acknowledgments

We thank Dr. June Wu, Department of Plastic Surgery, Columbia University, for her clinical comments on the manuscript. Ms. Sarah Kennedy is acknowledged for her technical assistance. We appreciate the administrative assistance of Janina Acloque, Zoila E. Noguerole and Maryann Wanner. This research was supported by NIH grants and DE015391 and DE013964 to J.J.M.

References

[1] Sekiya I, Larson BL, Smith JR, Pochampally R, Cui JG, Prockop DJ. Expansion of human adult stem cells from bone marrow stroma: conditions that maximize the yields of early progenitors and evaluate their quality. Stem Cells 2002;20:530–41.
[2] Caplan AI, Bruder SP. Mesenchymal stem cells: building blocks for molecular medicine in the 21st century. Trends Mol Med 2001;7:259–64.
[3] Baksh D, Song L, Tuan RS. Adult mesenchymal stem cells: characterization, differentiation, and application in cell and gene therapy. J Cell Mol Med 2004;8:301–16.
[4] Alhadlaq A, Mao JJ. Mesenchymal stem cells: isolation and therapeutics. Stem Cells Dev 2004;13:436–48.
[5] Shi YY, Nacamuli RP, Salim A, Longaker MT. The osteogenic potential of adipose-derived mesenchymal cells is maintained with aging. Plast Reconstr Surg 2005;116:1686–96.
[6] Alhadlaq A, Mao JJ. Tissue-engineered osteochondral constructs in the shape of an articular condyle. J Bone Joint Surg Am 2005;87: 936–44.
[7] Alhadlaq A, Mao JJ. Tissue-engineered neogenesis of human-shaped mandibular condyle from rat mesenchymal stem cells. J Dent Res 2003;82: 951–6.
[8] Atala A. Recent developments in tissue engineering and regenerative medicine. Curr Opin Pediatr 2006;18:167–71.
[9] Hollister SJ, Maddox RD, Taboas JM. Optimal design and fabrication of scaffolds to mimic tissue properties and satisfy biological constraints. Biomaterials 2002;23:4095–103.
[10] Longaker MT. Role of TGF-beta signaling in the regulation of programmed cranial suture fusion. J Craniofac Surg 2001;12:389–90.
[11] Mooney MP, Moursi AM, Opperman LA, Siegel MI. Cytokine therapy for craniosynostosis. Expert Opin Biol Ther 2004;4:279–99.
[12] Hong L, Mao JJ. Tissue-engineered rabbit cranial suture from autologous fibroblasts and BMP2. J Dent Res 2004;83:751–6.
[13] Mao JJ, Giannobile WV, Helms JA, Hollister SJ, Krebsbach PH, Longaker MT, et al. Craniofacial tissue engineering by stem cells. J Dent Res 2006;85:966–79.
[14] Marsh JL, Jenny A, Galic M, Picker S, Vannier MW. Surgical management of sagittal synostosis. A quantitative evaluation of two techniques. Neurosurg Clin N Am 1991;2:629–640.
[15] Tessier P. Autogenous bone grafts taken from the calvarium for facial and cranial applications. Clin Plast Surg 1982;9:531–8.
[16] De Pollack C, Renier D, Hott M, Marie PJ. Increased bone formation and osteoblastic cell phenotype in premature cranial suture ossification (craniosynostosis). J Bone Miner Res 1996;11:401–7.
[17] Chong SL, Mitchell R, Moursi AM, Winnard P, Losken HW, Bradley J, et al. Rescue of coronal suture fusion using transforming growth factor-beta 3 (Tgf-beta 3) in rabbits with delayed-onset craniosynostosis. Anat Rec A Discov Mol Cell Evol Biol 2003;274:962–71.
[18] Opperman LA, Moursi AM, Sayne JR, Wintergerst AM. Transforming growth factor-beta 3(Tgf-beta3) in a collagen gel delays fusion of the rat posterior interfrontal suture in vivo. Anat Rec 2002;267:120–30.
[19] Lenton KA, Nacamuli RP, Wan DC, Helms JA, Longaker MT. Cranial suture biology. Curr Top Dev Biol 2005;66:287–328.
[20] Baroni T, Lilli C, Marinucci L, Bellocchio S, Pezzetti F, Carinci F, et al. Crouzon's syndrome: differential in vitro secretion of bFGF, TGFbeta I isoforms and extracellular matrix macromolecules in patients with FGFR2 gene mutation. Cytokine 2002;19:94–101.
[21] Mao JJ, Nah HD. Growth and development: hereditary and mechanical modulations. Am J Orthod Dentofacial Orthop 2004;125:676–89.
[22] Moioli EK, Hong L, Guardado J, Clark PA, Mao JJ. Sustained release of TGFbeta3 from PLGA microspheres and its effect on early osteogenic differentiation of human mesenchymal stem cells. Tissue Eng 2006;12: 537–46.
[23] Collins JM, Ramamoorthy K, Da SA, Patston P, Mao JJ. Expression of matrix metalloproteinase genes in the rat intramembranous bone during postnatal growth and upon mechanical stresses. J Biomech 2005;38: 485–92.
[24] Marion NW, Mao JJ. Mesenchymal stem cells and tissue engineering. Methods Enzymol 2006;420:339–61.
[25] Alhadlaq A, Elisseeff JH, Hong L, Williams CG, Caplan AI, Sharma B, et al. Adult stem cell driven genesis of human-shaped articular condyle. Ann Biomed Eng 2004;32:911–23.
[26] Alhadlaq A, Tang M, Mao JJ. Engineered adipose tissue from human mesenchymal stem cells maintains predefined shape and dimension: implications in soft tissue augmentation and reconstruction. Tissue Eng 2005;11:556–66.
[27] Moss ML. Functional anatomy of cranial synostosis. Childs Brain 1975;1: 22–33.
[28] Zhang X, Kuroda S, Carpenter D, Nishimura I, Soo C, Moats R, et al. Craniosynostosis in transgenic mice overexpressing Nell-1. J Clin Invest 2002;110:861–70.
[29] Cohen Jr MM. Craniofacial disorders caused by mutations in homeobox genes MSX1 and MSX2. J Craniofac Genet Dev Biol 2000;20:19–25.
[30] Vij K, Mao JJ. Geometry and cell density of rat craniofacial sutures during early postnatal development and upon in vivo cyclic loading. Bone 2006;38:722–30.
[31] Roth DA, Longaker MT, McCarthy JG, Rosen DM, McMullen HF, Levine JP, et al. Studies in cranial suture biology: part I. Increased immunoreactivity for TGF-beta isoforms (beta 1, beta 2, and beta 3) during rat cranial suture fusion. J Bone Miner Res 1997;12:311–21.
[32] Krebsbach PH, Robey PG. Dental and skeletal stem cells: potential cellular therapeutics for craniofacial regeneration. J Dent Educ 2002;66:766–73.
[33] Harris MT, Butler DL, Boivin GP, Florer JB, Schantz EJ, Wenstrup RJ. Mesenchymal stem cells used for rabbit tendon repair can form ectopic bone and express alkaline phosphatase activity in constructs. J Orthop Res 2004;22:998–1003.
[34] Weng Y, Cao Y, Silva CA, Vacanti MP, Vacanti CA. Tissue-engineered composites of bone and cartilage for mandible condylar reconstruction. J Oral Maxillofac Surg 2001;59:185–90.
[35] Hung CT, Lima EG, Mauck RL, Takai E, LeRoux MA, Lu HH, et al. Anatomically shaped osteochondral constructs for articular cartilage repair. J Biomech 2003;36:1853–64.
[36] Martinek V, Latterman C, Usas A, Abramowitch S, Woo SL, Fu FH, et al. Enhancement of tendon-bone integration of anterior cruciate ligament grafts with bone morphogenetic protein-2 gene transfer: a histological and biomechanical study. J Bone Joint Surg Am 2002;84-A:1123–31.
[37] Spalazzi JP, Gallina J, Fung-Kee-Fung SD, Konofagou EE, Lu HH. Elastographic imaging of strain distribution in the anterior cruciate ligament and at the ligament-bone insertions. J Orthop Res 2006;24: 2001–10.
[38] Rahaman MN, Mao JJ. Stem cell-based composite tissue constructs for regenerative medicine. Biotechnol Bioeng 2005;91:261–84.
[39] Marie PJ, Coffin JD, Hurley MM. FGF and FGFR signaling in chondrodysplasias and craniosynostosis. J Cell Biochem 2005;96:888–96.
[40] Friedenstein AJ, Deriglasova UF, Kulagina NN, Panasuk AF, Rudakowa SF, Luria EA, et al. Precursors for fibroblasts in different populations of hematopoietic cells as detected by the in vitro colony assay method. Exp Hematol 1974;2:83–92.
[41] Opperman LA, Adab K, Gakunga PT. Transforming growth factor-beta 2 and TGF-beta 3 regulate fetal rat cranial suture morphogenesis by regulating rates of cell proliferation and apoptosis. Dev Dyn 2000;219: 237–47.

[42] Mao JJ. Mechanobiology of craniofacial sutures. J Dent Res 2002;81: 810–6.
[43] Peptan IA, Hong L, Evans CA. Multiple differentiation potentials of neonatal dura mater-derived cells. Neurosurgery 2007;60:346–52.
[44] Meikle MC, Heath JK, Hembry RM, Reynolds JJ. Rabbit cranial suture fibroblasts under tension express a different collagen phenotype. Arch Oral Biol 1982;27:609–13.
[45] Gabbay JS, Heller J, Spoon DB, Mooney M, Acarturk O, Askari M, et al. Noggin underexpression and runx-2 overexpression in a craniosynostosis rabbit model. Ann Plast Surg 2006;56:306–11.
[46] Quarto N, Longaker MT. FGF-2 inhibits osteogenesis in mouse adipose tissue-derived stromal cells and sustains their proliferative and osteogenic potential state. Tissue Eng 2006;12:1405–18.
[47] Warren SM, Brunet LJ, Harland RM, Economides AN, Longaker MT. The BMP antagonist noggin regulates cranial suture fusion. Nature 2003;422: 625–9.
[48] Zhang X, Cowan CM, Jiang X, Soo C, Miao S, Carpenter D, et al. Nell-1 induces acrania-like cranioskeletal deformities during mouse embryonic development. Lab Invest 2006;86:633–44.
[49] Ornitz DM, Marie PJ. FGF signaling pathways in endochondral and intramembranous bone development and human genetic disease. Genes Dev 2002;16:1446–65.
[50] Merrill AE, Bochukova EG, Brugger SM, Ishii M, Pilz DT, Wall SA, et al. Cell mixing at a neural crest-mesoderm boundary and deficient ephrin-Eph signaling in the pathogenesis of craniosynostosis. Hum Mol Genet 2006;15:1319–28.
[51] Moioli EK, Hong L, Mao JJ. Inhibition of osteogenic differentiation of human mesenchymal stem cells. Wound Repair Regen 2007;15: 413–21.
[52] Moioli EK, Clark PA, Xin X, Lal S, Mao JJ. Matrices and scaffolds for drug delivery in dental, oral and craniofacial tissue engineering. Adv Drug Deliv Rev 2007;59:308–24.